

Experimental Evaluation of Construction Waste and Ground Granulated Blast Furnace Slag as Alternative Soil Stabilisers

Umair Hasan · Amin Chegenizadeh ·
Mochamad Arief Budihardjo ·
Hamid Nikraz

Received: 24 April 2015 / Accepted: 16 January 2016 / Published online: 21 January 2016
© Springer International Publishing Switzerland 2016

Abstract In this study, the effect of ground granulated blast furnace slag (GGBFS) and recycled construction waste (CW) on bentonite clay stabilisation were investigated. The unconfined compressive strength (UCS) of specimens was evaluated with different combinations of GGBFS and CW over various curing periods. A series of micro analysis tests consisting of scanning electron microscope, energy dispersive spectrometer and X-ray diffraction were also conducted to determine the microstructural arrangement and mineralogical effect of the stabilisation treatment. The UCS results showed an increment in strength after introduction of GGBFS and CW and the longer curing period produced more pronounced results. The optimum additive ratio was calculated as 5 % of slag and 20 % of construction waste under all curing conditions. The micro analytical results also indicated formation of structural bonds between admixtures and bentonite in stabilised specimens, as slag crystals and bentonite particles were observed to occupy the cavities and vesicles on the construction

waste grains. However, the experimental data shows that the strength improvement is not significant with the addition of only construction waste.

Keywords Soil stabilisation · Bentonite · Slag · Construction waste · Unconfined compressive strength

1 Introduction

Several world regions, especially arid and semi-arid regions, are especially prone to comparatively large percentages of expansive soil compositions (Schanz and Elsayw 2015). The distinguishing feature of expansive soils is their ability to swell and shrink cyclically due to changes in the soil moisture content caused by changing environmental conditions. The expansion or shrinkage ability of the soil depends upon the clay mineralogy (Grim 1968; Cherian and Arnepalli 2015), particle composition and arrangement (Snethen et al. 1977), moisture content (MC), reduction of overburden stress and the presence of cations such as Na^+ , Ca^{2+} , Mg^{2+} and K^+ , which can result in the accumulation of large quantities of water in between the clay particles, causing the closely packed clay particles to drift apart (Mitchell and Raad 1973; Zhao et al. 2015).

There are various methods available to identify the shrink-swell potential of any specific type of soil, and the validity of the test results is largely based on the efficiency of the testing method. Similarly, there are several soil stabilisation approaches for countering the

U. Hasan (✉) · A. Chegenizadeh ·
M. A. Budihardjo · H. Nikraz
Department of Civil Engineering, Curtin University,
GPO Box U1987, Perth, WA 6845, Australia
e-mail: engruhasan@yahoo.com;
umair.hasan@postgrad.curtin.edu.au

M. A. Budihardjo
Department of Environmental Engineering, Diponegoro
University, Semarang, Indonesia

hazards presented by these soils, such as chemical, electrical, mechanical and thermal stabilisation (Hausmann 1990; Nicholson 2014). Conventional methods for the improvement of soil texture, plasticity and strength incorporate mechanical stabilisation through mixing of distinctive soils, surcharge loading, compaction-controlled replacement of soil and pre-wetting. Another technique is chemical stabilisation through the induction of particular proportions of additives like lime, fly ash, slag, cement and/or gypsum.

Chemical or additive stabilisation is one of the most commonly applied soil stabilisation methods. The treatment can be aimed at increasing soil particle size, reducing the plasticity index, enhancing strength, and decreasing the shrink-swell potential or cementation. It involves introducing one or more chemical compounds into the soil mass. Conventional compounds like cement and unconventional or recycled compounds such as slag, fly ash and lime have been effectively utilised for soil stabilisation (Phani Kumar and Sharma 2004; Al-Rawas et al. 2005; Neeraja and Rao Narsimha 2010; Yadu and Tripathi 2013; Khemissa and Mahamedi 2014; Ortega-López et al. 2014; Thyagaraj and Zodinsanga 2014).

The modernisation of architectural practices and industrialisation has led to large quantities of debris generated from the demolition of structures. This construction waste (CW) forms a major component of the solid waste in many countries, with only marginal quantities being utilised in backfilling on construction sites and the rest being mostly dumped on already scarce landfill sites. Therefore, construction waste causes land, resource and material depletion and deterioration (Behera et al. 2014; Wang et al. 2014). The Australian construction industry alone produces approximately 38 % waste for landfills each year (Schanz and Elsayy 2015).

Furthermore, many countries have problems with illegal or environmentally unsafe disposal of industrial by-products, for instance blast furnace slag. Globally growing concern over environmental safety has driven researchers worldwide to find more sustainable solutions to these problems and reuse waste materials. Similarly, researchers have also worked to find alternative materials for achieving soil stabilisation utilising several industrial by-products (Al-Malack et al. 2014; Amu et al. 2005; McCarthy et al. 2014).

Considering the huge imprint of construction activities on the environment (Horvath 2004), this research

work is focused on the use of recycled materials for soil stabilisation. The techniques of both chemical/additive stabilisation and mechanical composite stabilisation have been employed with GGBFS and construction waste as the soil stabilisers. Recycled construction waste (CW) has been preferred as the production of new aggregates increases CO₂ imprint (Limbachiya et al. 2012). These materials have already been used for reinforcement in various developed countries around Europe (Kasai 1989; Hansen 1986; Khalaf and DeVenny 2004; Poon and Chan 2007; Chakradhara Rao et al. 2011). The use of CW can not only reduce the carbon footprint of soil stabilisation but can produce better results in improving the bearing capacity of soft soils. Furthermore, the cost of procuring recycled, screened and sieved construction waste is extremely low in developed countries like Australia, for example in Western Australia, the screened construction waste only costs 8–10 AUD per tonne, and Commonwealth government provides incentives for greener construction practices like reuse of construction and demolition waste (Hyder Consulting 2011). This study had, therefore, been conducted to investigate the feasibility of utilising construction waste and GGBFS for the stabilisation of clay.

2 Materials and Methodology

2.1 Test Design

This study employed the techniques of both mechanical stabilisation through the induction of recycled construction waste, and chemical stabilisation by introducing GGBFS, in controlled proportions. The flowchart of the research work is presented in Fig. 1 and illustrates the soil treatment process.

2.2 Material and Sample Preparation

2.2.1 Clay

The clay selected for the purpose of this test was commercially manufactured bentonite procured from Sibelco Australia Limited. Other researchers have also used sodium bentonite in their investigation of expansive soils (Abdelrahman et al. 2013). The bentonite used was off-white in colour and had a fine powdered composition, as illustrated by Fig. 2a.

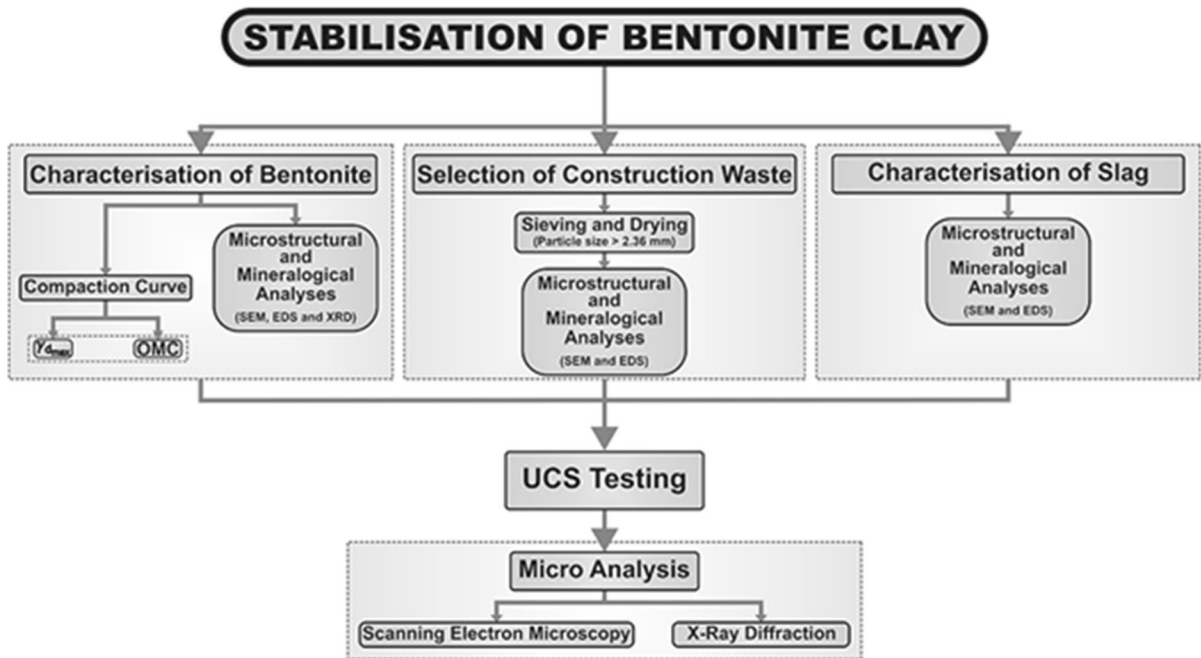


Fig. 1 Outline of research tests



Fig. 2 Test material images a bentonite clay, b construction waste, and c GGBFS

Bentonite has a specific gravity of 2.75 and is predominately composed of the smectite group of clay minerals (more than 74 %). Bentonite contains primarily fine Na-montmorillonite particles (surface area of 800 m²/kg) (National Research Council 2006). The particle size distribution of the bentonite is depicted in Fig. 3.

2.2.2 Construction and Demolition Waste

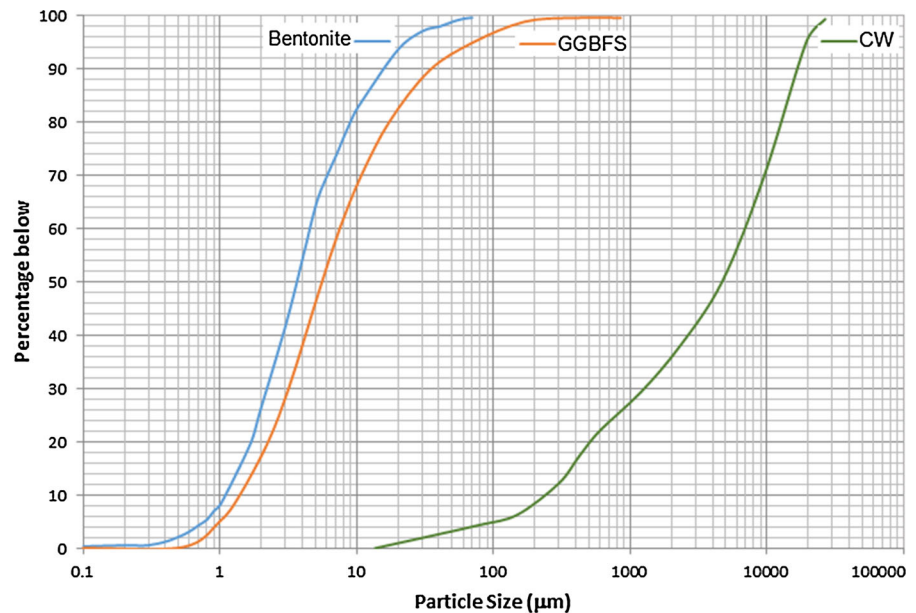
Construction waste (CW) was obtained from Capital Recycling Australia and mainly consisted of crushed concrete, tiles and masonry works that had been sieved by the supplier to remove the wood and glass residues.

The CW was stored in a reinforced plastic container. It was oven dried for 24 h at a temperature of 105 °C and sieved. The particles passing through sieve 4.75 mm and retained on sieve 2.36 mm were selected for the reason of this study. The particle size distribution of construction waste is presented in Fig. 3. The texture and element of the construction waste varied widely due to variations in the source materials, as shown in Fig. 2b.

2.2.3 Slag

The slag utilised for this study was ground granulated blast furnace slag (GGBFS) provided commercially by BGC Cement Australia Pty Limited. It generally has a

Fig. 3 Particle size distribution of the materials



glassy, fine and crystal-like texture as illustrated in Fig. 2c. The surface area of GGBFS is typically $>350 \text{ m}^2/\text{kg}$ (Siddique and Khan 2011; Al-Rawas et al. 2005). The particle size distribution of GGBFS is shown in Fig. 3.

GGBFS has mildly cementitious properties and is used with cement or lime (Higgins 2005). However, due to the hydraulic nature of the slag and the considerable presence of calcium, it may harden and hydrate without any additional material in the presence of water, even though the hydration process is considerably slower and may take considerable time to complete (Song et al. 2000). The chemical composition of GGBFS is provided in Fig. 4.

2.2.4 Sample Preparation

Different percentages of the two additives, GGBFS and CW, were used to separately investigate the influence of each additive on the UCS over a number of different curing periods. The sample combinations and the identified curing period are listed in detail in Table 1.

It should be noted at this stage that this research is part of an ongoing research on use of recycled materials for soil stabilisation and is intended to serve as foundation for further research using higher percentages of both additives. Lower CW proportions were chosen to prevent segregation of CW particles within the specimen matrix as the research focuses on the interlocking of

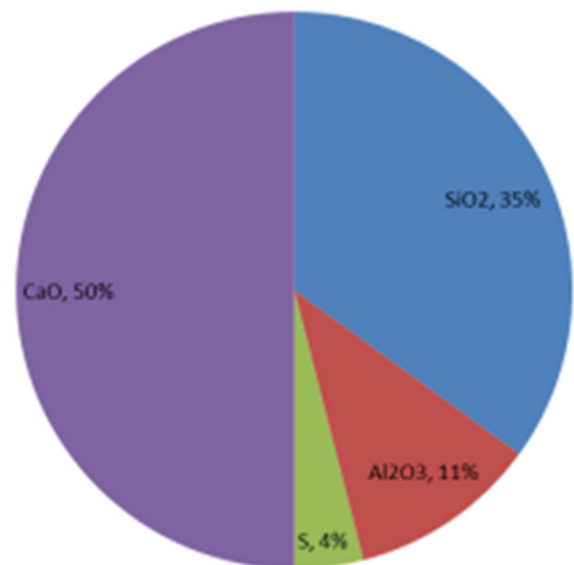


Fig. 4 Chemical composition of GGBFS provided by Cement Australia Pty Limited

construction grains with bentonite-GGBFS particles instead of other CW particles as the irregular shape may cause formation of small waterways within the specimen, thereby causing uneven water distribution. The optimum moisture content (OMC) by weight of the dry specimen was used for all the specimens to deduce comparative data for assessing the effects of the aforementioned two controlling factors. A manual

Table 1 Test specimen matrix

Curing periods (days)	1	3	7	14	21	28
Sample ID	Composition					
<i>Group 1</i>						
S1G1	100 % bentonite					
<i>Group 2</i>						
S1G2	2 % slag + 10 % CW + 88 % bentonite					
S2G2	2 % slag + 15 % CW + 83 % bentonite					
S3G2	2 % slag + 20 % CW + 78 % bentonite					
<i>Group 3</i>						
S1G3	3 % slag + 10 % CW + 87 % bentonite					
S2G3	3 % slag + 15 % CW + 82 % bentonite					
S3G3	3 % slag + 20 % CW + 77 % bentonite					
<i>Group 4</i>						
S1G4	4 % slag + 10 % CW + 86 % bentonite					
S2G4	4 % slag + 15 % CW + 81 % bentonite					
S3G4	4 % slag + 20 % CW + 76 % bentonite					
<i>Group 5</i>						
S1G5	5 % slag + 10 % CW + 85 % bentonite					
S2G5	5 % slag + 15 % CW + 80 % bentonite					
S3G5	5 % slag + 20 % CW + 75 % bentonite					

mixing technique was adapted to mix the additives into the soil mass. The mixtures were then prepared in a large tray by constantly spraying water at amounts calculated for the OMC through a spray bottle and mixing with the help of spatula till a homogeneous appearance was attained. Then the stabilised clay mixes were compacted in standard cylindrical steel moulds to produce specimens with dimensions of 10 cm × 20 cm under the standard compaction effort following Standards Australia AS 5101.4 (2008). The extracted specimens were then wrapped with thick plastic sheets and placed in a storage room for the respective curing periods to limit the effects of any external factors on the specimens. Bearing in mind that specimens were prepared by tamping at OMC; therefore the specimens were not saturated during UCS testing. Moreover, the UCS test has a limitation dealing with a fully saturated sample.

2.3 Laboratory Tests

2.3.1 Compressive Strength

The laboratory tests involved the investigation of the effects of stabilisers, GGBFS and construction waste, on the engineering behaviour of stabilised bentonite clay; for example, the unconfined compressive strength

(UCS) (see Fig. 5). The UCS tests were performed as per the Standards Australia AS 5101.4 (2008) specifications. The device used for this purpose is the GCTS Stress-Path Soil Triaxial System (STX-300) as shown in Fig. 5d. It has dedicated software in the attached computer interface, enabling control of the test parameters and results generation. An axial load was applied at the continuous rate of 1.0 ± 0.1 mm/min and the testing was stopped once the deformation had been recorded.

Figure 6 illustrates the unconfined compression of a typical test specimen. Once the load was applied, the specimen underwent deformation. A reduction in the length of the specimen was observed, whereas the cross-sectional area increased from 'A' to 'A'' under the influence of the applied compressive loading and the length changes from 'L' to 'L_o' after the ΔL change. The compressive strength of the specimen is associated with two parameters; the applied normal or axial compressive loading, 'P', and the surface area of the specimen where the load is being applied, which is dependent upon the diameter of the specimen.

2.3.2 Microanalysis

Microanalysis was performed to identify any changes in the elemental composition and physical appearance

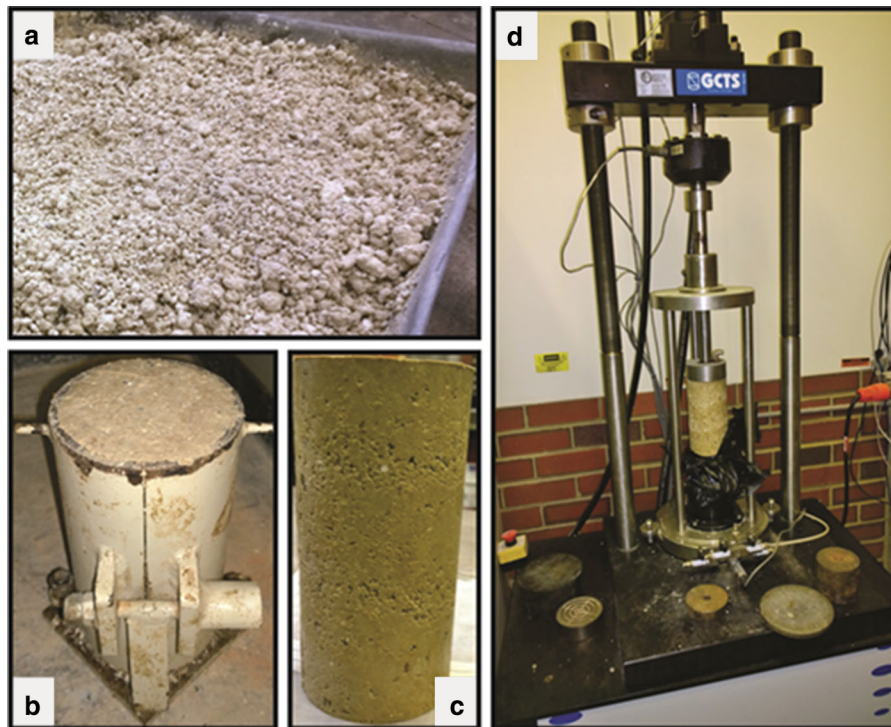


Fig. 5 UCS testing **a** prepared stabilised mixture, **b** specimen compaction, **c** stabilised specimen, and **d** STX-300 UCS test device

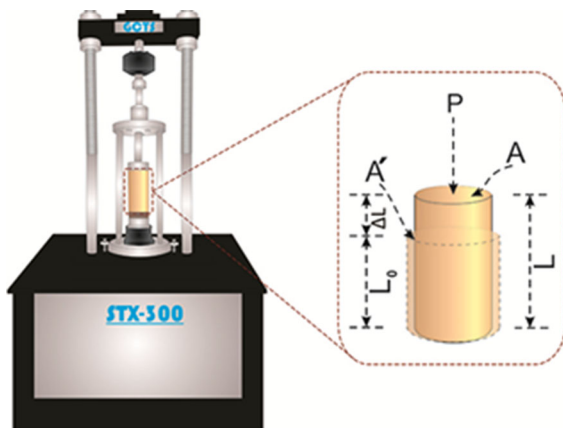


Fig. 6 Unconfined compression testing of soil specimen

of the bentonite after the action of the stabilisers. X-ray diffraction (XRD) graphs and scanning electron microscope (SEM) images were developed. The elemental distribution, morphology and arrangement at the microscale were analysed using a Zeiss Evo 40XVP SEM analysis device. This is also capable of performing energy dispersive spectrometer (EDS) analysis, among other functions. It is provided with a

dedicated computer and Oxford X-ray system controlled by INCA software. An electron beam with an acceleration voltage of 20 kV and a 100 μ A beam current was used with a 450 nm spot size and 8.5 mm working distance. X-ray diffraction quantitative analyses were carried out to determine the mineralogical characteristics of the test specimens using a Bruker-AXS D8 Advance Powder Diffractometer with Cu-K α X-ray radiation beam ($\lambda = 0.15404$ nm, voltage = 40 kV, current = 40 mA). 0.02 $^\circ$ /s was set as the scanning rate whereas the 2-theta data was collected in the 7.5 $^\circ$ –90 $^\circ$ area.

3 Results and Discussion

3.1 Material Microstructural and EDS Characterisation

3.1.1 Bentonite Clay

Figure 7 shows the SEM micromorphology of pure bentonite clay.

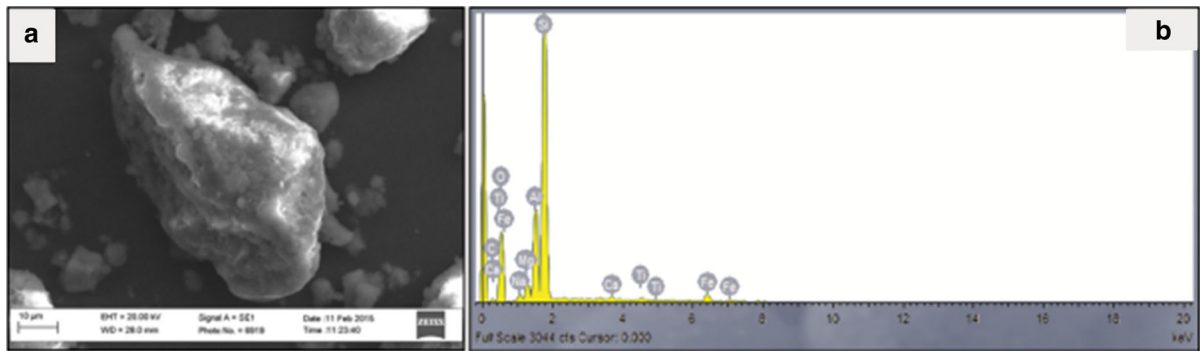


Fig. 7 Bentonite clay **a** SEM micrograph, and **b** EDS spectra

Table 2 Quantitative chemical composition of bentonite clay

Element	Weight%	Atomic%	k Ratio	Standard
O	62.07	75.21	0.34248	SiO ₂
Na	1.02	0.86	0.00604	Na ₂ O
Mg	1.7	1.35	0.01458	MgO
Al	6.35	4.56	0.0664	Al ₂ O ₃
Si	19.71	13.61	0.23039	SiO ₂
Ca	0.73	0.44	0.0089	CaO
Ti	7.51	3.63	0.11461	TiO ₂
Fe	0.26	0.11	0.00367	Fe ₂ O ₃
Totals	100			

The bentonite particles have amorphous crystallography as illustrated in Fig. 7a. The EDS spectra and results of the quantitative analysis of the bentonite particles are shown in Fig. 7b and Table 2.

Silicon and oxygen were observed to be the most dominant elements, followed by aluminium, sodium, titanium, magnesium, iron and calcium. The results indicate the presence of the montmorillonite-beidellite series (Deer et al. 2013).

3.1.2 GGBFS

Figure 8 displays the SEM micrograph and EDS spectra of the GGBFS used in this study.

As can be observed from the figure, the particles showed a definitive crystalline morphology. However, there was little uniformity in the shapes of the crystals. The observed particle sizes showed a varied size range of 30–45 μm .

The EDS spectra and results of the quantitative analysis of the GGBFS particles are summarised in Fig. 8b and Table 3. The results indicate a strong

presence of oxygen, with SiO₂ and MgO as the leading chemical compounds followed by aluminium, ferric and calcium oxides.

3.1.3 Construction Waste

Figure 9 illustrates the micromorphology of the construction waste particles. As can be seen, the construction waste particles have irregular or lenticular shapes (Fig. 9a). Fissures or vesicles and cracks were often found on the surfaces as is quite common with gravels and building aggregates, and this may have aided in the interlocking mechanism between the bentonite and construction waste particles.

The EDS spectra and quantitative data of the selected construction waste grains are displayed in Fig. 9b and Table 4. Since the construction waste contains a variety of materials such as crushed bricks, rubble, mortar etc., the elemental distribution may vary between the grains.

As the source of the grain is most likely crushed bricks, the quantitative chemical distribution indicates that these grains may belong to the large mineral family of plagioclase feldspars (Deer et al. 2013).

3.2 Standard Compaction Test

Bentonite was subjected to a standard compaction effort of 596 kJ/m³ as per Standards Australia AS 1289.5.4.2 (2007) to calculate the optimum moisture content (OMC) and the corresponding maximum dry density ($\gamma_{d_{max}}$). A compaction curve was plotted after a series of tests and the OMC and $\gamma_{d_{max}}$ were respectively obtained as 43 % and 1.08 g/cm³.

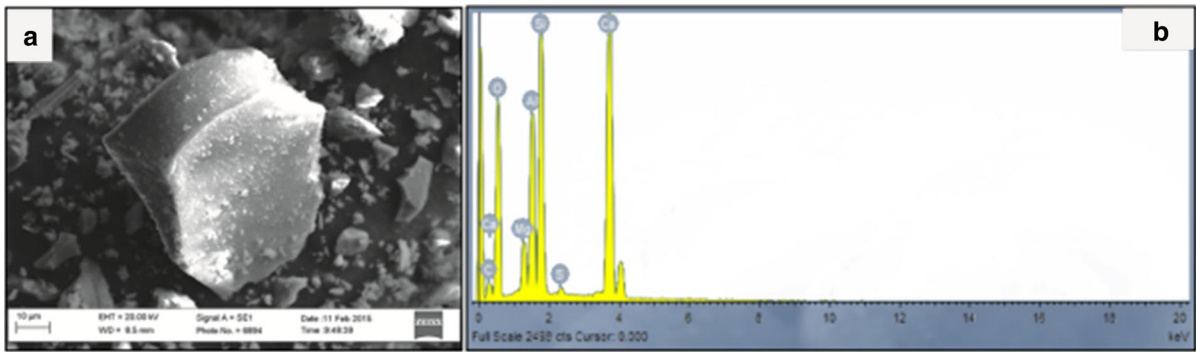


Fig. 8 GGBFS **a** SEM micrograph, and **b** EDS spectra

Table 3 Quantitative chemical composition of GGBFS

Element	Weight%	Atomic%	k Ratio	Standard
O	53.02	69.27	0.17233	SiO ₂
Mg	2.8	2.4	0.02271	MgO
Al	8.47	6.56	0.08227	Al ₂ O ₃
Si	13.84	10.3	0.14747	SiO ₂
S	0.43	0.28	0.0051	FeS ₂
Ca	21.45	11.19	0.31293	CaO
Totals	100			

3.3 Unconfined Compressive Strength

Unconfined compressive strength is essentially a parameter of stabilisation process efficiency which is defined as the maximum unit stress calculated after subjecting the stabilised specimens to a monotonic axial load. The deformation was mainly observed through the formation of minor cracks on the outer shell of the specimen which widened until specimen failure was observed. Figure 10 shows the failure

mechanism of the test specimens. This phenomenon is a common failure mechanism of ductile materials during unconfined compression.

A strength development index (SDI) was introduced as a non-dimensional parameter to easily quantify the effect of each of the controlling factors, i.e. the effect of the percentage of each additive and the curing time on the UCS of the stabilised soil. It is defined as:

$$SDI_{n_{curing, \% \text{ additives}}} = \frac{UCS \text{ of the stabilised soil specimen}}{UCS \text{ of the unstabilised soil specimen}} \geq 1$$

where ‘n’ corresponds to either of the controlling factors, representing either the percentage of the two stabilising additives in the mixture or the number of days the specimen has been subjected to the curing conditions. The lower limit of ‘1’ indicates that the addition of any admixture should not result in a decrement in the UCS. A similar parameter has also been proposed by Saride et al. (2013).

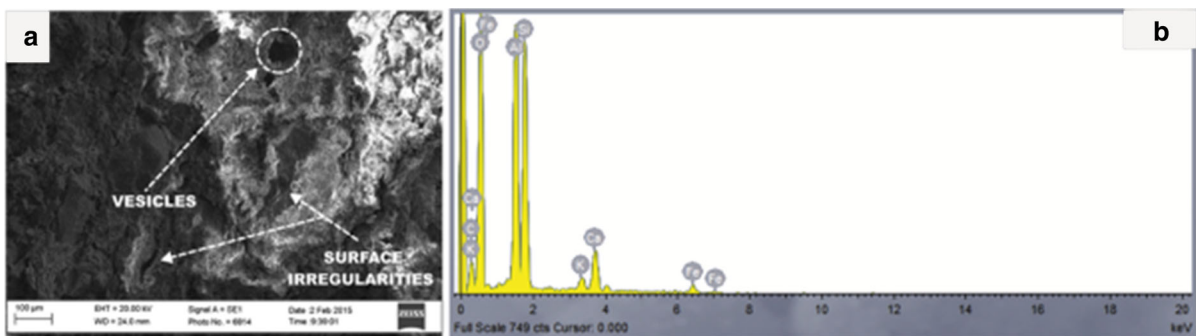
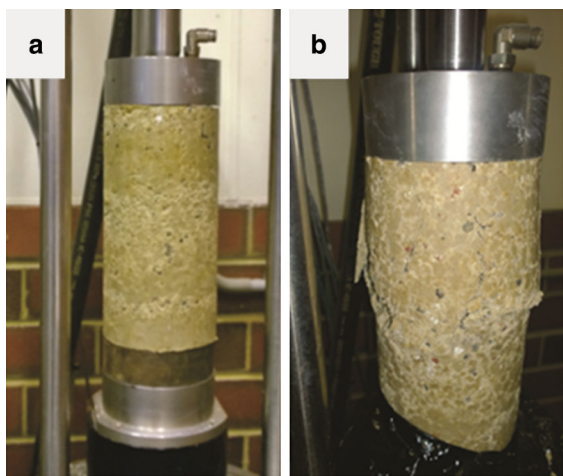


Fig. 9 Construction waste **a** SEM micrograph, and **b** EDS spectra

Table 4 Quantitative chemical composition of construction waste

Element	Weight%	Atomic%	k Ratio	Standard
O	48.44	62.65	0.20718	SiO ₂
Na	0.82	0.74	0.00444	Na ₂ O
Mg	1.61	1.37	0.0123	MgO
Al	9.51	7.29	0.08597	Al ₂ O ₃
Si	35.18	25.91	0.33002	SiO ₂
K	1.5	0.8	0.0164	K ₂ O
Ca	1	0.52	0.01152	CaO
Fe	1.94	0.72	0.02208	Fe ₂ O ₃
Totals	100			

**Fig. 10** Specimen failure mechanism **a** undeformed specimen, **b** deformed specimen

3.3.1 Initial Strength of the Untreated Specimen

The stress–strain relationship of pure bentonite is illustrated in Fig. 11 for the different curing periods investigated in this research. Test results suggest that although both specimens showed a slight variation in the failure strain, little or no strength development was observed for the unstabilised soil specimens for different curing periods. The maximum compressive strength of the untreated bentonite was found to be 76.71 kPa.

3.3.2 Effect of Curing Time on Stabilised Compacted Soil

The curing time of the additive-stabilised bentonite specimens was among one of the primary control

factors. The evolution of the unconfined strength of the stabilised specimens throughout the final curing period of 28 days is illustrated in Figs. 12, 13 and 14 for different proportions of both additives.

The UCS results for the construction waste and bentonite blended specimens with increasing percentages of slag show the development of strength with curing. The effect was more noticeable in the initial periods of curing with all of the specimens gaining at least 75 % of the strength increment by the 14th day of curing. Although further curing resulted in an increase in strength values, the effect was not as prominent as for the 14 day curing period. The effect of curing became more noticeable as the percentage of additives, specifically GGBFS, was increased. This might have been due to the cementitious nature of the slag and its slower hydration reaction. Even though GGBFS reacts with water to show hydration or pozzolanic behaviour, the process is fairly negligible at the lower slag percentages. For the specimen S1G2, the UCS only showed an increment of approximately 2.79 % between the 1st and 3rd day of sample curing. However, specimen S1G4 exhibited strength improvement of 3.97 % and S1G5 corresponded to UCS development of 5.03 %, between the same curing days. Further curing resulted in the improvement of the UCS value and optimum values were reached after 28 days of curing for all specimen, therefore, showing inclination in the UCS versus curing period graphs for all test specimens. As shown in Fig. 12, for specimen S2G3, the 28th day cured specimen showed a UCS value of approximately 160.65 kPa which was 46.98 % higher than that noted after 1 day of specimen curing. Although the hydration reaction of the stabilising GGBFS might have continued after the 28th day of curing (Kim et al. 2011), the construction waste grains tend to produce little effect with each successive curing day, and may have showed a negligible increase in the compressive strength of the stabilised mixture over time.

3.3.3 Effect of Additives

Each of the additives produced different effects on the UCS of the stabilised mix for the same curing period. The effect of each additive is discussed separately.

3.3.3.1 Effect of Slag It was observed that for all combinations of additives, the maximum strength was achieved in the 28 day curing period. This finding

Fig. 11 Stress-strain curves of pure bentonite for 7 and 28 day curing periods

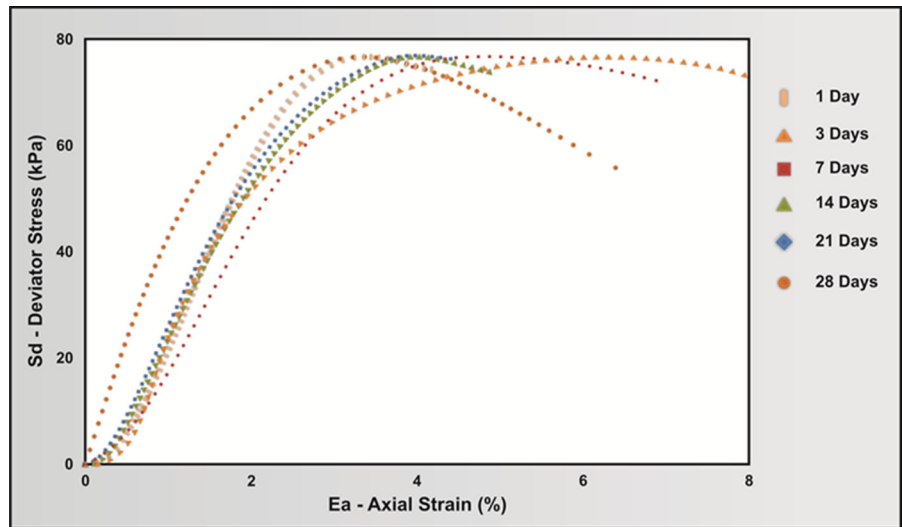


Fig. 12 Evolution of UCS with curing time for 2–5 % slag and 10 % construction waste

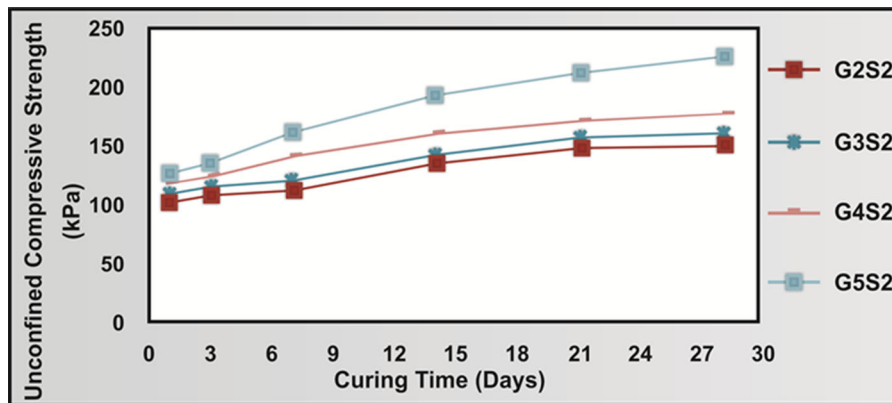
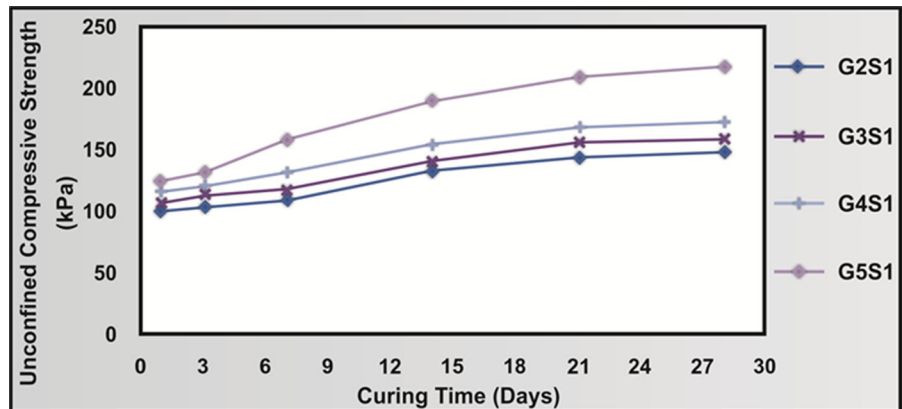
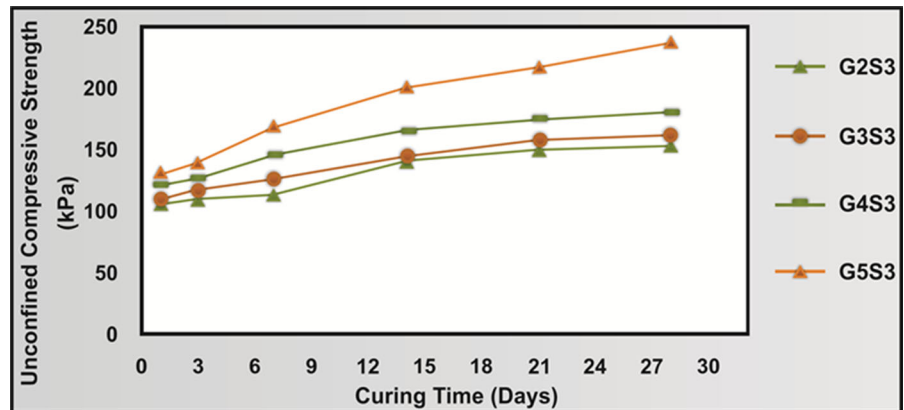


Fig. 13 Evolution of UCS with curing time for 2–5 % slag and 15 % construction waste

Fig. 14 Evolution of UCS with curing time for 2–5 % slag and 20 % construction waste



shows that the cementitious nature of GGBFS plays a vital role in the development of compressive strength. It can be seen in Fig. 15 that the addition of GGBFS alone has shown increasing trends of the compressive strength of the bentonite.

It was also observed that the increase in UCS value with the increment in the proportion of GGBFS only grew by 15 % when the percentage of GGBFS was increased from 2 to 3 % for 28 days of curing, SDI_{28} of 1.92 to SDI_{28} of 2.07 respectively for the 10 % proportion of the construction waste. Conversely, a higher increment in the strength was observed when the percentage of slag was further increased. The SDI_{28} value rose by a factor of 0.19, corresponding to a 19.27 % rise when the GGBFS percentage was increased from 3 to 4 % for a construction waste content of 10 %. Furthermore, an increase of 0.58 was documented in SDI_{28} , being a sharp 58.16 % rise when the GGBFS proportion was further increased to 5 % for the same percentage of construction waste. One of the reasons behind this observation could be the unavailability of sufficient slag particles within the specimen matrices for the purpose of hydration to form stronger structural bonds in form of silicates or cementitious hydration compounds such as portlandite. The maximum increase after 1 day of curing was observed for the specimen G5S3 which had an SDI_1 of 1.71. However, further curing resulted in a sharper increase in the compressive strength, where a maximum strength of 236.93 kPa was observed for the specimen G5S3 ($SDI_{28} = 3.09$).

3.3.3.2 Effect of Construction Waste Figure 16 shows the development of compressive strength with increasing percentages of the selected gradation of construction waste over a 28 day curing period.

The increase in the UCS of the stabilised bentonite clay specimens was observed to be directly correlated with the proportion of the demolition and construction waste in the mixture. After the first day of curing (Fig. 13), the UCS of the stabilised specimen with the least amount of slag, i.e. 2 %, was seen to grow by an SDI factor of 0.03 from $SDI_2 \text{ } \% \text{ GGBFS} + 10 \% \text{ CW} = 1.31$, corresponding to a strength of 100.82 kPa, to $SDI_2 \text{ } \% \text{ GGBFS} + 15 \% \text{ CW} = 1.34$ (UCS = 103.07 kPa), with a 5 % increment in the amount of inducted construction waste. A further increase of 5 % yielded an increase in the SDI by a factor of 0.04 which produced a UCS value of 106 kPa. Further strength increment was observed with the lengthening curing periods, because of the GGBFS cementitious nature, and the effects of the increased percentage of construction waste in the stabilised mixture were more pronounced with the high percentages of GGBFS in the treated specimens. This statement was reconfirmed, as after the curing of the stabilised specimens for 28 days (Fig. 16), the UCS value was found to have increased from 147.93 to 150.67 kPa, which shows an SDI increment from $SDI_2 \text{ } \% \text{ GGBFS} + 10 \% \text{ CW} = 1.93$ to $SDI_2 \text{ } \% \text{ GGBFS} + 15 \% \text{ CW} = 1.96$. Upon addition of another 5 % of construction waste, the UCS value rose slightly to 153.09 kPa, corresponding to $SDI_2 \text{ } \% \text{ GGBFS} + 20 \% \text{ CW} = 1.99$. However, the contribution of the construction waste alone without any GGBFS addition seems to have a minor effect on the UCS value of the bentonite.

3.3.4 Optimum Strength Improvement

Figure 17 shows the strength development indices of all of the treated specimens for the 28 day curing

Fig. 15 Evolution of UCS with GGBFS addition with different construction waste percentages over a 28 day curing period

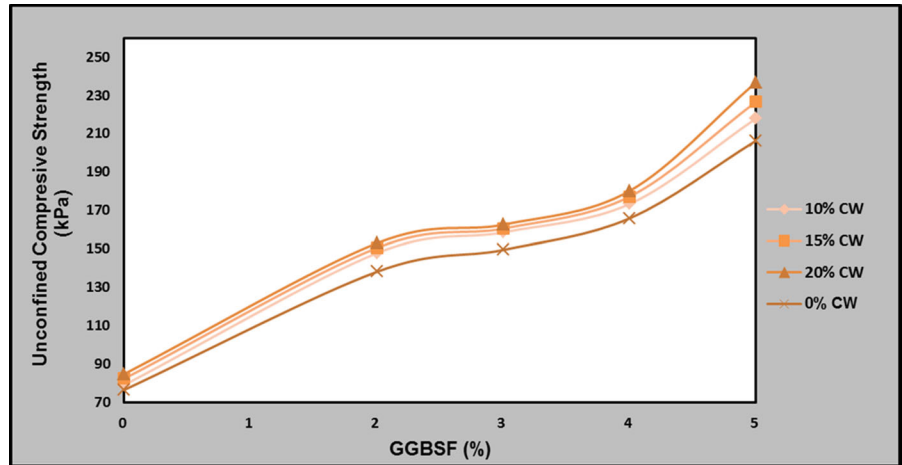


Fig. 16 Evolution of the UCS of construction waste for different GGBFS concentrations after 28 days of curing

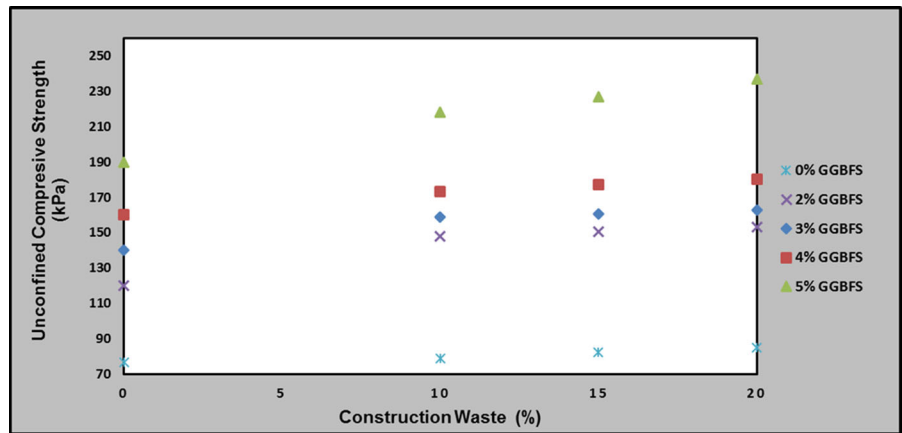
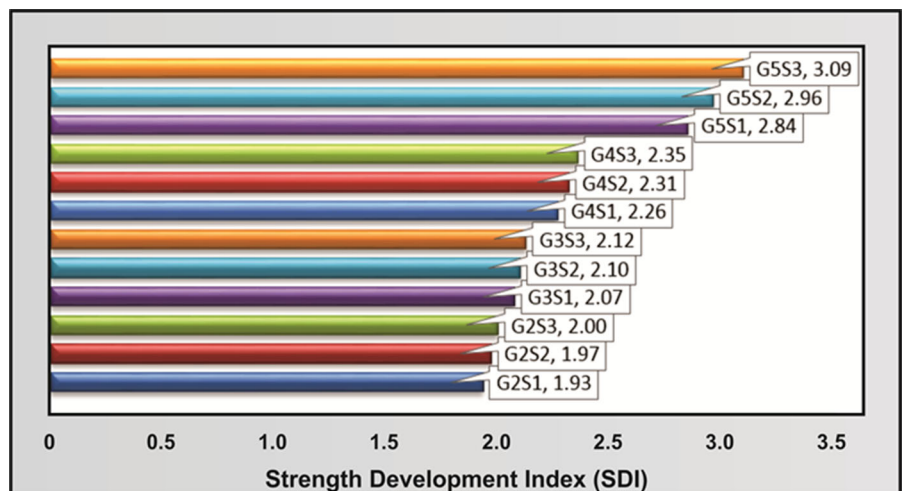


Fig. 17 SDI for 28 days curing (SDI₂₈)



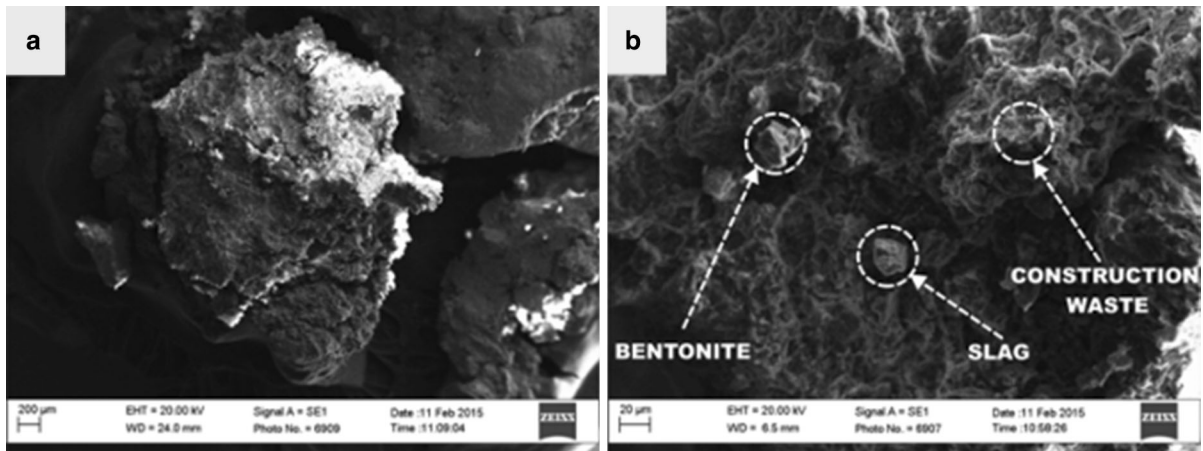


Fig. 18 SEM micrograph of a **a** completely covered, and **b** partially covered specimen from G5S3 after 28 days of curing

period, as the maximum strength for all admixture-stabilised bentonite specimens was observed after the specimens had been cured for 28 days. The maximum strength after the 28 day curing period was observed for specimen G5S3, which contained 5 % slag and 20 % construction waste, being SDI_5 % GGBFS + 20 % CW = 3.09. This shows that stabilised soil strength grew by almost 209 %, while the least strength development was observed for specimen G2S1 which contained the lowest percentages of additives.

Since all admixture-stabilised bentonite specimen was prepared by tamping at OMC therefore the effect of saturation condition was not targeted in this study. In addition, this study is based on the certain period of curing time, considering possibility of stabilized clay becomes saturated after long time of submergence, further investigation is required in order to generalise the UCS result.

3.4 Microanalysis of Materials

3.4.1 SEM Microstructural and EDS

Characterisation of Post-28 Days G5S3

Figure 18 shows the SEM micrographs of the stabilised specimen G5S3. This specimen contains 5 % GGBFS and 20 % construction waste added to the bentonite clay.

In general, the bentonite grains and the GGBFS crystals occupied the fissures and cavities of the construction waste particles as illustrated in Fig. 18.

Figure 19 summarises the results of the quantitative analysis and the EDS spectra of the stabilised specimen G5S3. Figure 19a shows silicon and oxygen to be the most dominant elements, followed by magnesium, iron, calcium and aluminium. The cations were observed to be bonded with their oxides. These results are quite similar to the SEM and EDS results for GGBFS. Figure 19b EDS and SEM results are consistent with the chemical composition and crystallography results for bentonite which indicated a higher percentage of montmorillonite. The results shown in Fig. 19c are quite similar to those for the quantitative analysis of the construction waste grains as shown in Fig. 9 and Table 4.

3.4.2 Mineralogical XRD Analysis

In addition to the SEM and EDS analyses on the material morphology and mineralogy, the diffraction bands of the untreated bentonite clay were used to understand the presence of different minerals and to obtain benchmark data for comparing the effects of the two stabilising agents on the virgin clay. The results of the XRD test on untreated bentonite clay are presented in Fig. 20b.

The XRD characterisation results illustrated the dominance of clay minerals such as quartz [SiO_2], illites [$K_{1.5-1.0}Al_4[Si_{6.5-7.0}Al_{1.5-1.0}O_{20}](OH)_4$], alkali feldspars [(K, Na)[$AlSi_3O_8$]], mica [$AlSi_2O_6(OH)_2$] and kaolinites [$Al_4[Si_4O_{10}](OH)_8$] (Deer et al. 2013) This confirms the findings from the EDS tests which also showed SiO_2 as the major component of the

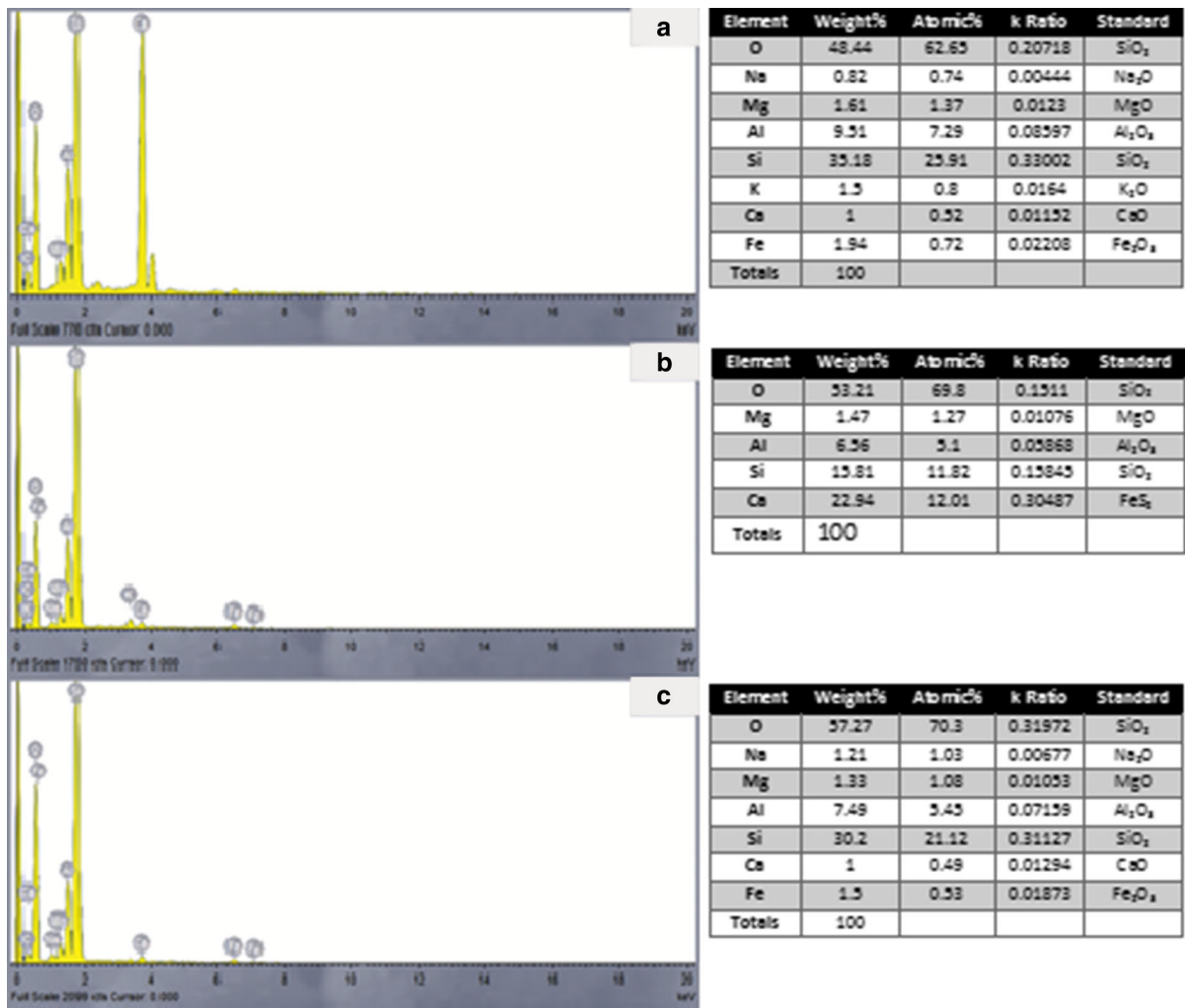


Fig. 19 EDS spectra and quantitative data for S3G5 after 28 days of curing with **a** GGBFS, **b** bentonite, and **c** construction waste grains

bentonite clay. These XRD test results also show a similarity to the results of tests previously conducted on bentonite clay from a similar source (Amiralian et al. 2015).

Figure 20 illustrates the X-ray diffraction (XRD) spectrum for the stabilised soil specimen G5S3 after 28 days of curing alongside the XRD for untreated bentonite clay, so as to gain further insight into the crystallography and mineralogy of the treated and untreated specimens. The specimen was selected based upon the SDI criterion as it showed a maximum SDI value ($SDI_{28} = 3.09$), indicating that the maximum strength had been achieved for this specimen. The peaks of the XRD diffraction bands indicate that the

tested stabilised mixture showed similar peaks overall, with slight variation resulting from the formation of cementitious compounds (Fig. 20a). Calcium hydroxide $Ca(OH)_2$ was found, which might have formed as a result of the hydration of calcium oxide (Birss and Thorvaldson 1955).

4 Conclusion

A series of unconfined compressive strength (UCS) tests was performed to investigate the effect GGBFS and construction and demolition waste for stabilisation of bentonite clay. The results showed that both

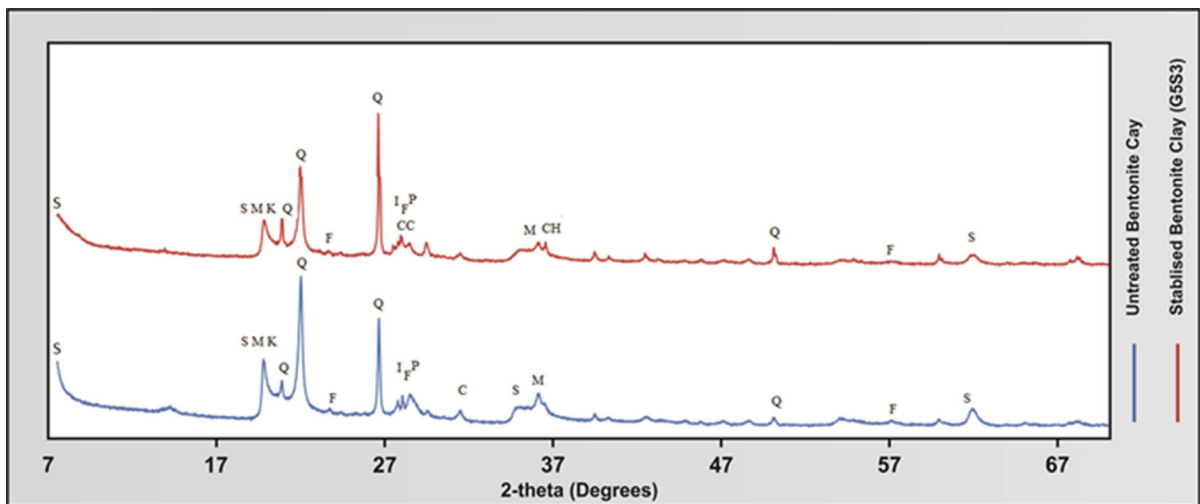


Fig. 20 X-ray diffraction spectrum of **a** stabilised soil specimen (G5S3) after 28 days of curing, and **b** untreated bentonite clay (*S* smectite, *M* mica, *K* kaolinite, *Q* quartz, *F* feldspar, *I* illite, *CC* calcium carbonate, *P* plagioclase, *CH* calcium hydroxide, *C* calcite)

additives have diverse contribution for the stabilisation purposes. The UCS values for the treated specimens insignificantly increased from 124.77 to 127 kPa when the CW proportion was increased from 10 to 15 % for the 1 day curing period. Another 5 % addition of the construction waste also led to very little increment of UCS value of 131.42 kPa. However, the evolution of the UCS with increasing stabiliser proportions was influenced by the curing periods. The optimum results for all combinations were obtained after the curing period of 28 days. It was observed that the UCS value for the bentonite clay specimen stabilised with 5 % slag and 20 % construction waste grew from 131.42 kPa after 1 day of curing, to 236.93 kPa after 28 days of curing. This corresponds to the maximum strength improvement observed in the treated specimens and showed a 209.09 % increase from the initial untreated specimen strength. Meanwhile, the XRD results indicated that the presence of moisture in the mixture resulted in changes in the mineralogical composition of the stabilised mixtures with $\text{Ca}(\text{OH})_2$ formation due to the hydration of CaO . The outcome of the experimental study showed that the compressive strength of the bentonite increases along with GGBFS addition. However, the addition of construction waste alone did not significantly increase the compressive strength of the bentonite clay.

Acknowledgments The authors acknowledge the use of Curtin University's Microscopy and Microanalysis Facility,

whose instrumentation has been partially funded by the University, State and Commonwealth Governments.

References

- Abdelrahman GE, Mohamed HK, Ahmed HM (2013) New replacement formations on expansive soils using recycled EPS beads. In: Proceedings of 18th ICSMGE
- Al-Malack MH, Abdullah GM, Baghabra Al-Amoudi OS, Bukhari AA (2014) Stabilization of indigenous Saudi Arabian soils using fuel oil flyash. *J King Saud Univ Eng Sci*. doi:10.1016/j.jksues.2014.04.005
- Al-Rawas AA, Hago AW, Al-Sarmi H (2005) Effect of lime, cement and Sarooj (artificial pozzolan) on the swelling potential of an expansive soil from Oman. *Build Environ* 40(5):681–687. doi:10.1016/j.buildenv.2004.08.028
- Amiralian S, Budihardjo MA, Chegenizadeh A, Nikraz H (2015) Study of scale effect on strength characteristic of stabilised composite with sewage sludge—part A: preliminary study. *Constr Build Mater* 80:339–345. doi:10.1016/j.conbuildmat.2014.07.117
- Amu OO, Fajobi AB, Afekhuai SO (2005) Stabilizing potential of cement and fly ash mixture on expansive clay soil. *J Appl Sci* 5(9):1669–1673
- Behera M, Bhattacharyya SK, Minocha AK, Deoliya R, Maiti S (2014) Recycled aggregate from C&D waste & its use in concrete—a breakthrough towards sustainability in construction sector: a review. *Constr Build Mater* 68:501–516. doi:10.1016/j.conbuildmat.2014.07.003
- Birss FW, Thorvaldson T (1955) The mechanism of the hydration of calcium oxide. *Can J Chem* 33(5):881–886. doi:10.1139/v55-106
- Chakradhara Rao M, Bhattacharyya SK, Barai SV (2011) Influence of field recycled coarse aggregate on properties of concrete. *Mater Struct* 44(1):205–220. doi:10.1617/s11527-010-9620-x

- Cherian C, Arnepalli DN (2015) A critical appraisal of the role of clay mineralogy in lime stabilization. *Int J Geosynth Ground Eng* 1(1):1–20. doi:[10.1007/s40891-015-0009-3](https://doi.org/10.1007/s40891-015-0009-3)
- Deer WA, Howie RA, Zussman J (2013) An introduction to the rock-forming minerals, 3rd edn. Mineralogical Society of Great Britain & Ireland, London
- Grim RE (1968) Clay mineralogy, 2nd edn. McGraw-Hill, New York
- Hansen TC (1986) Recycled aggregates and recycled aggregate concrete second state-of-the-art report developments 1945–1985. *Mater Struct* 19(3):201–246. doi:[10.1007/BF02472036](https://doi.org/10.1007/BF02472036)
- Hausmann MR (1990) Engineering principles of ground modification. McGraw-Hill, New York
- Higgins DD (2005) Soil stabilisation with ground granulated blastfurnace slag. UK Cementitious Slag Makers Association (CSMA) report. Surrey
- Horvath A (2004) Construction materials and the environment. *Annu Rev Environ Resour* 29(1):181–204. doi:[10.1146/annurev.energy.29.062403.102215](https://doi.org/10.1146/annurev.energy.29.062403.102215)
- Hyder Consulting (2011) Construction and Demolition Waste Status Report Environment Department of Sustainability, Water, Population and Communities and Queensland Department of Environment and Resource Management. <http://www.environment.gov.au/system/files/resources/323e8f22-1a8a-4245-a09c-006644d3bd51/files/construction-waste.pdf>
- Kasai Y (1989) The Second International RILEM Symposium on demolition and reuse of concrete and masonry. *Mater Struct* 22(4):312–319. doi:[10.1007/BF02472565](https://doi.org/10.1007/BF02472565)
- Khalaf F, DeVenny A (2004) Recycling of demolished masonry rubble as coarse aggregate in concrete: review. *J Mater Civ Eng* 16(4):331–340. doi:[10.1061/\(ASCE\)0899-1561\(2004\)16:4\(331\)](https://doi.org/10.1061/(ASCE)0899-1561(2004)16:4(331))
- Khemissa M, Mahamedi A (2014) Cement and lime mixture stabilization of an expansive overconsolidated clay. *Appl Clay Sci* 95:104–110. doi:[10.1016/j.clay.2014.03.017](https://doi.org/10.1016/j.clay.2014.03.017)
- Kim HS, Park JW, An YJ, Bae JS, Han C (2011) Activation of ground granulated blast furnace slag cement by calcined alunite. *Mater Trans* 52(2):210–218
- Limbachiya M, Meddah MS, Ouchagour Y (2012) Use of recycled concrete aggregate in fly-ash concrete. *Constr Build Mater* 27(1):439–449. doi:[10.1016/j.conbuildmat.2011.07.023](https://doi.org/10.1016/j.conbuildmat.2011.07.023)
- McCarthy MJ, Csetenyi LJ, Sachdeva A, Dhir RK (2014) Engineering and durability properties of fly ash treated lime-stabilised sulphate-bearing soils. *Eng Geol* 174:139–148. doi:[10.1016/j.enggeo.2014.03.001](https://doi.org/10.1016/j.enggeo.2014.03.001)
- Mitchell TK, Raad L (1973) Control of volume changes in expansive earth materials. Workshop on Expansive Clays and Shales in Highway Design and Construction, Denver, Colorado: Frost I Jord/Norway
- National Research Council (2006) Geological and geotechnical engineering in the new millennium: opportunities for research and technological innovation. The National Academies Press, Washington, DC
- Neeraja D, Rao Narsimha AV (2010) Use of certain admixtures in the construction of pavement on expansive clayey subgrade. *Int J Eng Sci Technol* 2(11):6108–6114
- Nicholson PG (2014) Soil improvement and ground modification methods. Butterworth-Heinemann, Oxford
- Ortega-López V, Manso JM, Cuesta II, González JJ (2014) The long-term accelerated expansion of various ladle-furnace basic slags and their soil-stabilization applications. *Constr Build Mater* 68:455–464. doi:[10.1016/j.conbuildmat.2014.07.023](https://doi.org/10.1016/j.conbuildmat.2014.07.023)
- Phani Kumar BR, Sharma RS (2004) Effect of fly ash on engineering properties of expansive soils. *J Geotech Geoenviron Eng* 130(7):764–767
- Poon CS, Chan D (2007) The use of recycled aggregate in concrete in Hong Kong. *Resour Conserv Recycl* 50(3):293–305. doi:[10.1016/j.resconrec.2006.06.005](https://doi.org/10.1016/j.resconrec.2006.06.005)
- Saride S, Puppala AJ, Chikyal SR (2013) Swell-shrink and strength behaviors of lime and cement stabilized expansive organic clays. *Appl Clay Sci* 85:39–45. doi:[10.1016/j.clay.2013.09.008](https://doi.org/10.1016/j.clay.2013.09.008)
- Schanz T, Elsayy MBD (2015) Swelling characteristics and shear strength of highly expansive clay–lime mixtures: a comparative study. *Arab J Geosci* 8(10):7919–7927. doi:[10.1007/s12517-014-1703-5](https://doi.org/10.1007/s12517-014-1703-5)
- Siddique R, Khan MI (2011) Supplementary cementing materials. Vol. 37, Engineering materials. Springer, Berlin
- Snethen DR, Johnson LD, Patrick DM (1977) An evaluation of expedient methodology for identification of potentially expansive soils. US Army Engineer Waterways Experiment Station, USAEWES, Vicksburg, Mis. Report No. FHWA-RD-77-94
- Song S, Sohn D, Jennings HM, Mason TO (2000) Hydration of alkali-activated ground granulated blast furnace slag. *J Mater Sci* 35(1):249–257. doi:[10.1023/A:1004742027117](https://doi.org/10.1023/A:1004742027117)
- Standards Australia AS 1289.5.4.2 (2007) Methods of testing soils for engineering purposes—soil compaction and density tests—compaction control test—assignment of maximum dry density and optimum moisture content values
- Standards Australia AS 5101.4 (2008) Methods for preparation and testing of stabilized materials—unconfined compressive strength of compacted materials
- Thyagaraj T, Zodinanga S (2014) Laboratory studies on stabilization of an expansive soil by lime precipitation technique. *J Mater Civ Eng* 24(8):1067–1075. doi:[10.1061/\(ASCE\)MT.1943-5533.0000483](https://doi.org/10.1061/(ASCE)MT.1943-5533.0000483)
- Wang J, Li Z, Tam VWY (2014) Critical factors in effective construction waste minimization at the design stage: a Shenzhen case study, China. *Resour Conserv Recycl* 82:1–7. doi:[10.1016/j.resconrec.2013.11.003](https://doi.org/10.1016/j.resconrec.2013.11.003)
- Yadu L, Tripathi RK (2013) Effects of granulated blast furnace slag in the engineering behaviour of stabilized soft soil. *Procedia Eng* 51:125–131. doi:[10.1016/j.proeng.2013.01.019](https://doi.org/10.1016/j.proeng.2013.01.019)
- Zhao H, Liu J, Guo J, Zhao C, Gong B (2015) Reexamination of lime stabilization mechanisms of expansive clay. *J Mater Civ Eng* 27(1):04014108. doi:[10.1061/\(ASCE\)MT.1943-5533.0001040](https://doi.org/10.1061/(ASCE)MT.1943-5533.0001040)